Published in Langmuir 13, issue 8, pp. 2363–2372, 1997,
which should be used for any reference to this work

Organized Molecular Films from New Ferrocene-Containing Molecular Units

Robert Deschenaux,*,† Sonia Megert,† Cornélia Zumbrunn,† Jurgen Ketterer,‡ and Rolf Steiger†,‡

Institut de Chimie, Universite´ de Neucha^tel, Av. de Bellevaux 51, 2000 Neucha^tel, Switzerland, and Ilford AG, 1723 Marly, Switzerland

The design and synthesis of new amphiphilic ferrocene derivatives and their capability for forming Langmuir and Langmuir−Blodgett films are reported. The film formation at the air−water interface was followed by surface pressure−molecular area isotherm, surface potential−molecular area isotherm, and Brewster angle microscopy. The stability and structure of the transferred films were investigated by UV−vis spectroscopy and small angle X-ray experiments. Transfer ratios near unity were obtained. Two hydrophobic alkyl chains combined with either one or two hydrophilic functions gave stable and ordered films. One hydrophobic alkyl chain associated to one hydrophilic headgroup required the presence of an intercalant for obtaining organized molecular films. This behavior clearly illustrated the key role played by the three-dimensional structure of the ferrocene unit which tends to decrease the intermolecular interactions because of its bulkiness; this is in agreement with results reported for ferrocene-containing thermotropic liquid crystals (Deschenaux, R.; Goodby, J. W. In *Ferrocenes: Homogeneous Catalysis, Organic Synthesis, Materials Science*; Togni, A., Hayashi, T. Eds.; VCH Verlagsgesellschaft: Weinheim, 1995; pp 471−495).

Introduction

The organization of amphiphilic ferrocene derivatives at the air−water interface and into Langmuir−Blodgett (LB) films generated enthusiastic studies, such as photoinduced electron transfer,[1] interfacial electrochemistry,[2] surface potential measurements,[3] polarized spectroscopic characterizations[4] and photopolymerization.[5] From a technological viewpoint, these investigations are of fundamental importance as the incorporation of the redox-active ferrocene unit into organized molecular films is expected to lead to a source of new anisotropic materials with the view to developing miniaturized electronic devices.[6]

The successful design and building of ordered two- and three-dimensional films with desired properties require that, for a specific molecular unit, the structural parameters (size, shape, conformation, configuration, hydrophilic−hydrophobic balance) which govern its organization be known. In the case of ferrocene, no detailed investigation was carried out to bring to the fore the *structure−supramolecular organization* relationship, especially concerning the role played by the three-dimensional structure of the metallocene core. This lack of information hindered, at least in part, a complete exploitation of the properties of ferrocene for generating organized molecular films with tailor-made properties.

We describe, herein, new symmetrically and unsymmetrically substituted amphiphilic ferrocene derivatives and their capability for forming monolayers at the air−water interface and LB films. We also emphasize the role played by the three-dimensional structure of the ferrocene core on the formation and stability of the monolayers. The search for new substitution patterns which may open the doors toward novel and less conventional structures motivated the present work.

Chart 1

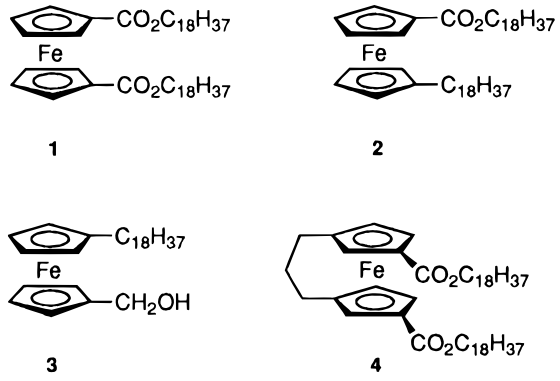

Results and Discussion

Design. The investigated ferrocene derivatives are shown in Chart 1. Diester **1** was selected in view of published data which showed that stable films could be prepared from 1,1'-disubstituted ferrocene derivatives[7] (diamides, [Fe{(η^5-C_5H_4)$CONHC_nH_{2n+1}$}$_2$]; diesters, [Fe{(η^5-C_5H_4)$OOCC_nH_{2n+1}$}$_2$]). Compound **1** represents the structure from which all other ferrocene derivatives were designed. Ferrocene derivative **2** was prepared to explore the influence of the number of hydrophilic functions in disubstituted systems (**1**, two hydrophilic groups; **2**, one hydrophilic group). Ferrocene **3** was designed to emphasize the influence of the number of hydrophobic alkyl chains with respect to the number of hydrophilic groups (**1**, two hydrophilic groups and two hydrophobic chains;

* To whom correspondence should be addressed: Fax, (++41) 32 718 25 11; e-mail, robert.deschenaux@ich.unine.ch.
† Université de Neuchâtel.
‡ Ilford AG.

⊗ Abstract published in *Advance ACS Abstracts* April, 1, 1997.

(1) Fujihira, M.; Sakomura, M. *Thin Solid Films* **1989**, *179*, 471.
(2) (a) Aoki, A.; Miyashita, T. *Macromolecules* **1996**, *29*, 4662. (b) Lindholm-Sethson, B.; Orr, J. T.; Majda, M. *Langmuir* **1993**, *9*, 2161.
(3) Lindholm-Sethson, B.; Åberg, S. *Langmuir* **1995**, *11*, 1244.
(4) Hsu, Y.; Penner, T. L.; Whitten, D. G. *Langmuir* **1994**, *10*, 2757.
(5) Fukuda, A.; Koyama, T.; Hanabusa, K.; Shirai, H.; Nakahara, H.; Fukuda, K. *J. Chem. Soc., Chem. Commun.* **1988**, 1104.
(6) Fujihira, M. In *Nanostructures Based on Molecular Materials*; Göpel, W., Ziegler, Ch., Eds; VCH Verlagsgesellschaft: Weinheim, 1992; pp 27−46.
(7) (a) Nakahara, H.; Katoh, T.; Sato, M.; Fukuda, K. *Thin Solid Films* **1988**, *160*, 153. (b) Nakahara, H.; Fukuda, K.; Sato, M. *Thin Solid Films* **1985**, *133*, 1.

Scheme 1[a]

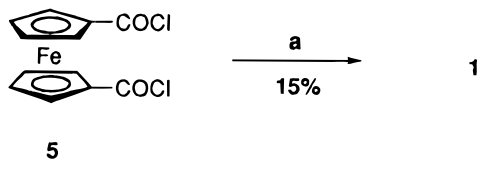

[a] (a) $C_{18}H_{37}OH$, Et_3N, 4-pyrrolidinopyridine, CH_2Cl_2, room temperature, 16 h.

2, one hydrophilic group and two hydrophobic chains; **3**, one hydrophilic group and one hydrophobic chain). Ferrocenophane derivative **4** was synthesized to emphasize a possible influence of the ferrocene conformation: compounds **1**−**3** can adopt different conformations while for **4** rotation is prevented because of the trimethylene bridge between the two cyclopentadienyl rings. The 1,1',3,3'-substitution pattern (see numbering in Chart 2 inserted in the Experimental Section) was selected because in this case the two ester functions stand apart from the trimethylene bridge and can both interact with the water surface.

Syntheses. Diester **1** was prepared by reacting ferrocene-1,1'-diacid chloride **5**[8] with octadecanol in CH_2Cl_2 at room temperature (Scheme 1).

The synthesis of **2** is outlined in Scheme 2. Treatment of acid chloride derivative **6**[8] with benzyl alcohol gave protected ester **7**. The latter was acylated with stearoyl chloride (→**8**) under Friedel−Crafts reaction conditions. Alkyl derivative **9** was obtained by reduction of the acyl function. Removal of the benzyl protective group under standard hydrogenation conditions led to acid intermediate **10** which was transformed into the corresponding acid chloride **11** with oxalyl chloride. Esterification of **11** with octadecanol furnished the targeted ferrocene derivative **2**.

The preparation of **3** is shown in Scheme 3. Acid chloride **6**[8] was esterified with methanol to give **12**. Acylation of the latter with stearoyl chloride under Friedel−Crafts conditions led to **13**, which was subsequently transformed into alkyl derivative **14**. Reduction of the ester function gave the desired amphiphile **3**.

[3]Ferrocenophane **4** was prepared as described in Scheme 4. Treatment of a mixture of mono- (not shown here) and diacid chlorides **15**[9] with lithium octadecanoate, obtained by reacting octadecanol with butyllithium, gave a mixture of mono- and diesters. Targeted compound **4** was isolated and purified by column chromatography. Its structure was confirmed by mass spectrometry, ^1H NMR, ^{13}C NMR, ^{13}C APT (attached proton test), and short and long range HETCOR (heteronuclear correlation) spectroscopy.

Film Formation at the Air−Water Interface. The formation of the Langmuir films at the air−water interface was investigated by means of surface pressure−molecular area isotherm, surface potential-molecular area isotherm, and Brewster angle microscopy (BAM). BAM images are reported for **1** and **2**; the other ferrocene derivatives gave similar results.

Diester **1** showed typical behavior of amphiphiles at the air−water interface. The surface pressure *versus* molecular area isotherm confirmed the formation of a stable monolayer (Figure 1). A phase transition was observed between 30 and 40 mN/m. The extrapolated molecular area of $A_o = 0.42$ nm^2/molecule corresponded to the value expected for a two-chain amphiphile[7] and confirmed the obtention of a dense monolayer. Further information concerning the behavior of **1** during the film formation was obtained from BAM (Figure 2). As a consequence of hydrophobic intermolecular interactions, a phase already formed at very low surface pressure (Figure 2a). On further compressing, two phases were detected from the presence of white and black zones (Figure 2b). When the surface pressure was further raised, the black areas decreased in number and dimensions (Figure 2c) and disappeared at 25 mN/m (Figure 2d), which resulted in the presence of a unique phase. The anisotropy

Scheme 2[a]

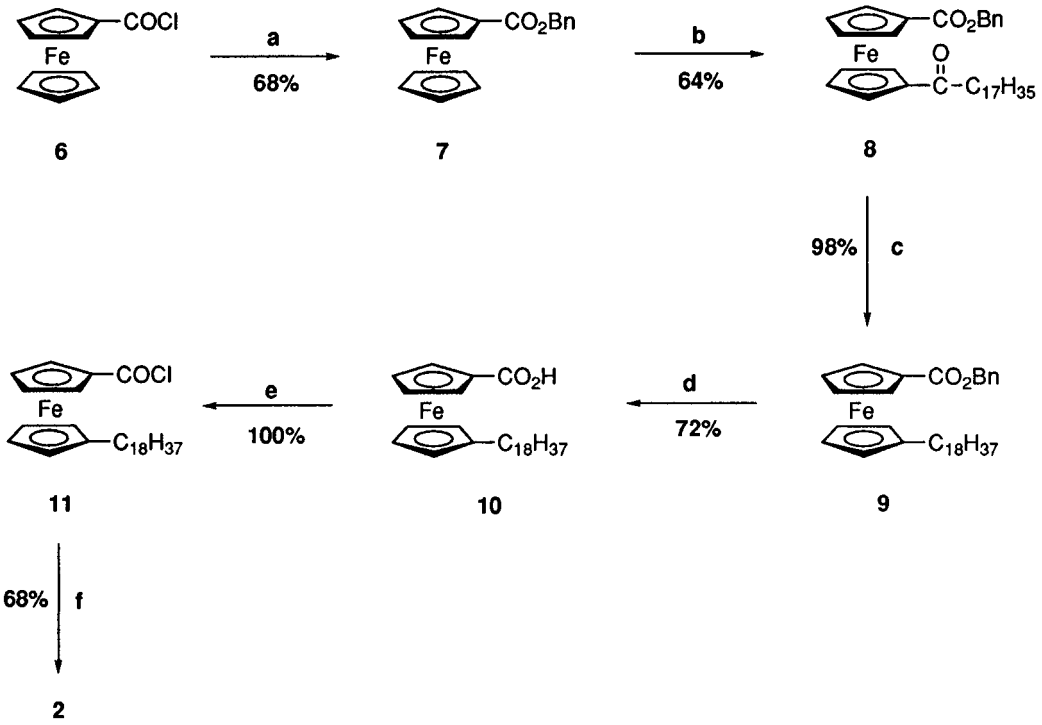

[a] (a) Benzylalcohol, Et_3N, CH_2Cl_2, room temperature, 4 h. (b) $C_{17}H_{35}COCl$, Zn, $AlCl_3$, CH_2Cl_2, 0 °C, 2 h. (c) Zn, $HgCl_2$, H_2O, concentrated HCl, toluene, reflux, 24 h. (d) H_2, Pd/C, CH_2Cl_2, room temperature, 4 h. (e) Oxalyl chloride, pyridine, CH_2Cl_2, reflux, 5 h. (f) $C_{18}H_{37}OH$, Et_3N, 4-pyrrolidinopyridine, CH_2Cl_2, reflux, overnight.

Scheme 3[a]

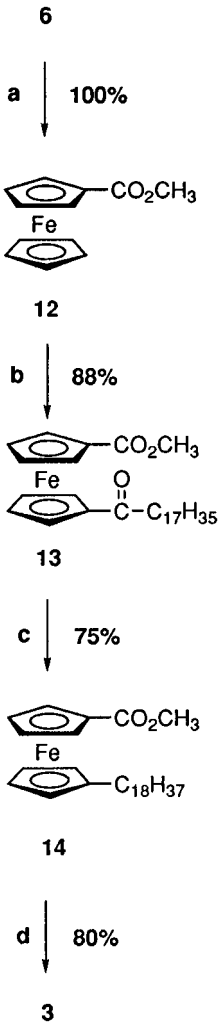

[a] (a) CH_3OH, Et_3N, 4-pyrrolidinopyridine, CH_2Cl_2, reflux, 3 h. (b) $C_{17}H_{35}COCl$, Zn, $AlCl_3$, CH_2Cl_2, 0 °C, 3 h. (c) Zn, $HgCl_2$, H_2O, concentrated HCl, toluene, reflux, 3 h. (d) $LiAlH_4$, THF, 0 °C, 30 min.

Scheme 4[a]

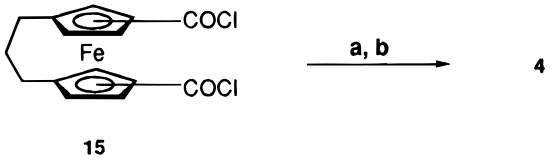

[a] (a) $C_{18}H_{37}OLi$, THF, room temperature (1 h), then reflux (2 h). (b) Column chromatography (silica gel, pentane/diethyl ether 9:1). The yield of the reaction cannot be given because the ratio of mono- and diacid chlorides in the starting material is unknown.

of the latter phase was confirmed by changing the angle of the polarizor (compare part d with parts e and f of Figure 2 which represent the layer at the same surface pressure but with different polarizor angle). At 45 mN/m, *i.e.*, after the phase transition, a more compact phase was obtained (Figure 2g). This phase transition was supported by the fact that a variation of the polarizor angle had no influence on the BAM image. From a surface pressure of *ca.* 62 mN/m collapse of the film was observed (Figure 2h).

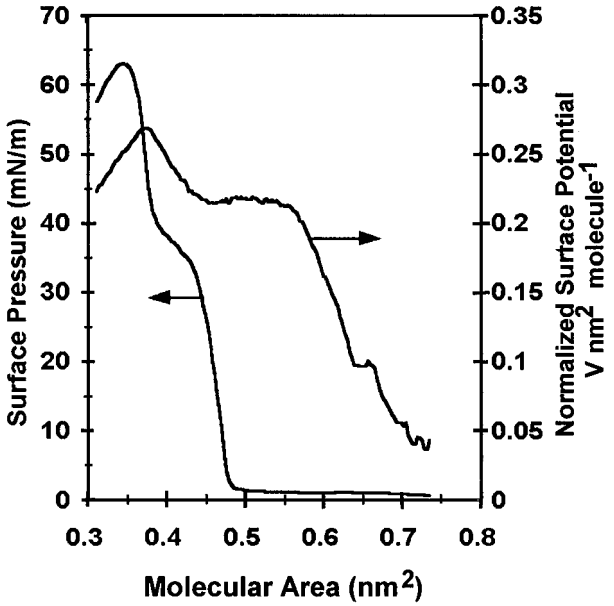

Figure 1. Surface pressure and normalized surface potential *versus* molecular area isotherms of **1** on aqueous NaCl (10^{-3} M) subphase at 25 °C (the formation of the short plateau at *ca.* 0.1 V nm^2 molecule^{-1} was not reproducible and was attributed to the passage of a less ordered liquid expanded zone under the electrode).

The variation of the surface pressure *versus* molecular area isotherm indicated that compression of **2** gave a stable film (Figure 3). No phase transition was observed. The extrapolated molecular area (0.43 nm^2/molecule) was in agreement with the behavior of a two-chain amphiphile. BAM revealed (i) the formation of domains at low surface pressure (Figure 4a), (ii) the formation of a homogeneous film during increase of the surface pressure (Figure 4b), and (iii) collapse of the film at *ca.* 60 mN/m (Figure 4c).

The data obtained for **1** and **2** indicated that combination of two hydrophobic chains with either one or two hydrophilic functions led to substitution patterns capable of forming stable and ordered Langmuir films at the air–water interface.

No stable monolayer was obtained with **3**, compression of which led to a slow increase of the surface pressure until *ca.* 25 mN/m (Figure 5) which corresponded to the collapse pressure as visualized by BAM (not shown here). In comparison with the data of **1** and **2**, the behavior observed from **3** (and from other ferrocene derivatives analogous to **3** differentiating from the polar headgroup)[10] indicated that one alkyl chain is less favorable than two for obtaining stable Langmuir films. This result can be explained in terms of structural considerations. The ferrocene core is a bulky three-dimensional moiety.[11] If it is substituted by one long chain, the space around the ferrocene is filled only partially. Consequently, weak intermolecular interactions take place between the ferrocenes, leading to unstable films.

From the results obtained for **1** and **2**, we anticipated that addition of 1 equiv of octadecane to the solution of ferrocene **3** used for spreading may restore favorable interactions between the molecular units: octadecane would play the role of an intercalant and replace the second alkyl chain as in **1** or **2**. This was in fact what we obtained from a **3**/octadecane (1:1 molar ratio) mixture as shown in Figure 6. A sharp increase of the surface pressure *versus* molecular area isotherm was observed which indicated

(8) Knobloch, F. W.; Rauscher, W. H. *J. Polym. Sci.* **1961**, *54*, 651.
(9) (a) Werner, A.; Friedrichsen, W. *J. Chem. Soc., Chem. Commun.* **1994**, 365. (b) Hillman, M.; Matyevich, L.; Fujita, E.; Jagwani, U.; McGowan, J. *Organometallics* **1982**, *1*, 1226.
(10) Deschenaux, R.; Megert, S.; Zumbrunn, C. Unpublished results.
(11) Elschenbroich C.; Salzer, A. In *Organometallics*; VCH Verlagsgesellschaft: Weinheim, 1992.

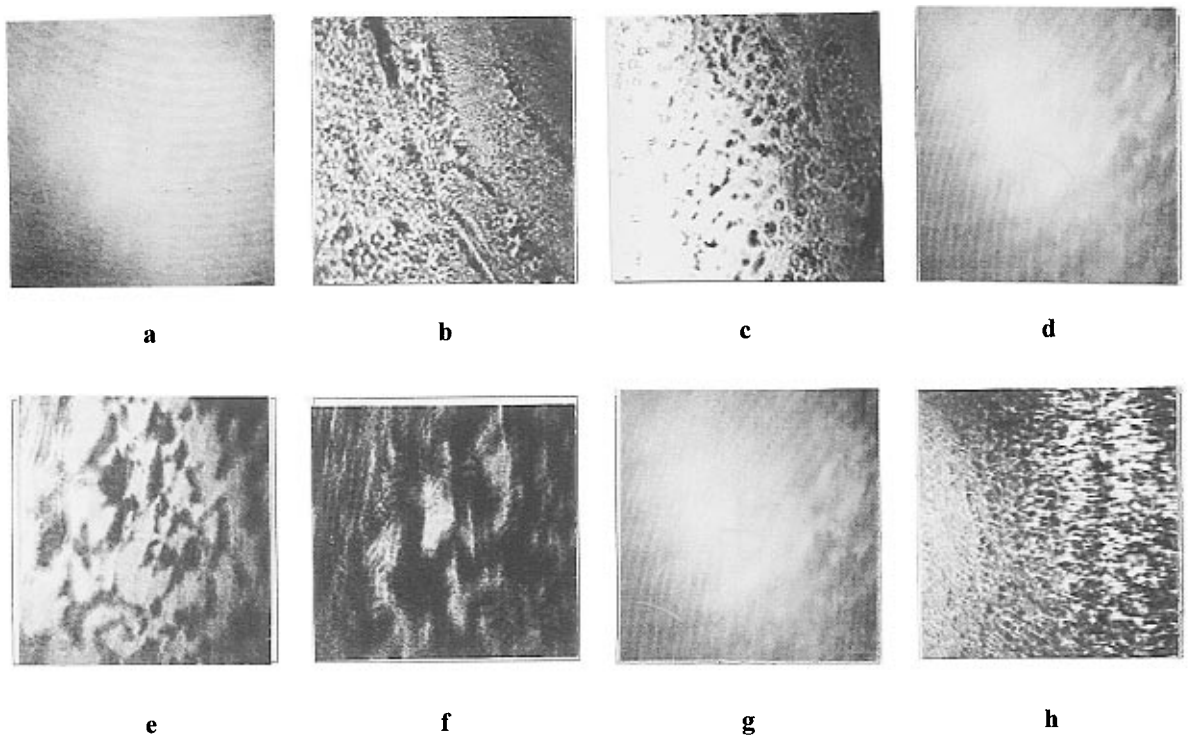

Figure 2. Brewster angle microscopy during compression of **1** (see Figure 1) on pure water at 25 °C at a surface pressure of (a) 0 mN/m (A > 1.5 nm^2/mol), (b) 0 mN/m (A = 0.8 nm^2/mol), (c) 4 mN/m, (d) 25 mN/m (polarizor position 0°), (e) 25 mN/m (polarizor position 100°), (f) 25 mN/m (polarizor position −80°), (g) 45 mN/m, and (h) > 60 mN/m (magnification: horizontally, 0.95 cm = 100 μm; vertically, 0.7 cm = 100 μm).

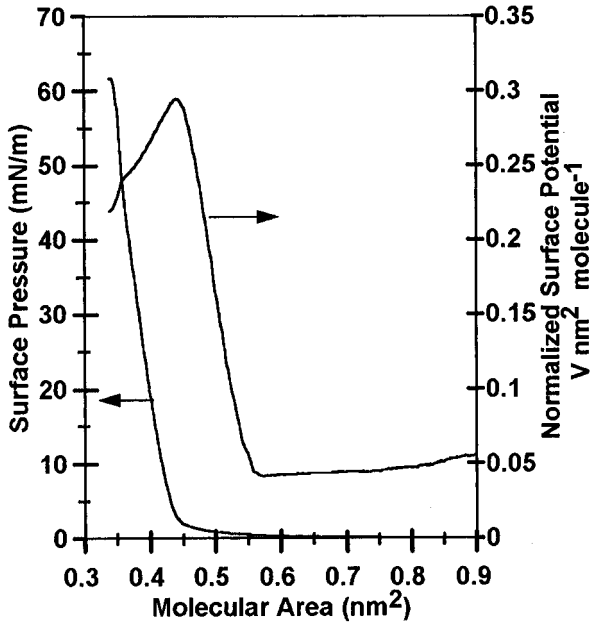

Figure 3. Surface pressure and normalized surface potential *versus* molecular area isotherms of **2** on aqueous NaCl (10^{-3} M) subphase at 20 °C (similar behavior was observed at 25 °C).

that a stable and ordered film formed. The extrapolated molecular area A_o = 0.42 nm^2/molecule was in agreement with a two-chain substituted ferrocene. BAM (not shown here) confirmed the formation of a homogeneous film between 0.30 and 0.45 nm^2.

Interestingly, the behavior observed for **3** and **3**/octadecane is in agreement with studies conducted with ferrocene-containing thermotropic liquid crystals which demonstrated that, as a consequence of stronger intermolecular interactions,[12] disubstituted ferrocene derivatives present a higher mesomorphism than monosubstituted ones.

The compression isotherm of ferrocenophane **4** is shown in Figure 7. Because of the additional substituent bridging the two cyclopentadienyl rings, a larger extrapolated molecular area was obtained for **4** (A_o = 0.51 nm^2/molecule) than for **1**, **2**, and **3**/octadecane.

The variation of the normalized surface potential as a function of molecular area was recorded for **1**, **2**, and **3**/octadecane (Figures 1, 3, and 6). The same conclusions can be drawn from the surface pressure and normalized surface potential isotherms. In the case of **1**, the normalized surface potential isotherm shows three regions: (1) between 0.70 and 0.55 nm^2 corresponding to the formation of a stable and ordered monolayer; (2) between 0.55 and 0.45 nm^2 (plateau region) which may reflect a reorganization of the molecules within the Langmuir film; (3) from *ca*. 0.45 nm^2 corresponding to the collapse of the monolayer. For **2** and **3**/octadecane only two regions are observed: an increase followed by a decrease of the normalized surface potential indicating formation and collapse of the monolayer, respectively.

Complementary experiments were performed to check the stability of the monolayers. Firstly, the stability was examined by recording the barrier motion at a constant surface pressure. For **1** (25 mN/m, *i.e.*, transfer pressure), **2** (20 mN/m, *i.e.*, transfer pressure), and **3**/octadecane (30 mN/m, *i.e.*, transfer pressure), a variation of ±0.1 mm/min was detected. In the case of **4** (from 15 to 55 mN/m), a variation of ±0.2 mm/min was always obtained. Secondly, the ferrocene derivatives were compressed at different rates (5, 10, 15, 20, 25, and 30 mm/min). Similar compression isotherms were obtained for **1**, **2**, and **3**/octadecane. In the case of **4**, a variation of the compression speed led to differences in the compression isotherm. These observations confirmed that stable monolayers were obtained from **1**, **2**, and **3**/octadecane

(12) Deschenaux, R.; Goodby, J. W. In *Ferrocenes: Homogeneous Catalysis, Organic Synthesis, Materials Science;* Togni, A., Hayashi, T., Eds.; VCH Verlagsgesellschaft: Weinheim, 1995; pp 471−495.

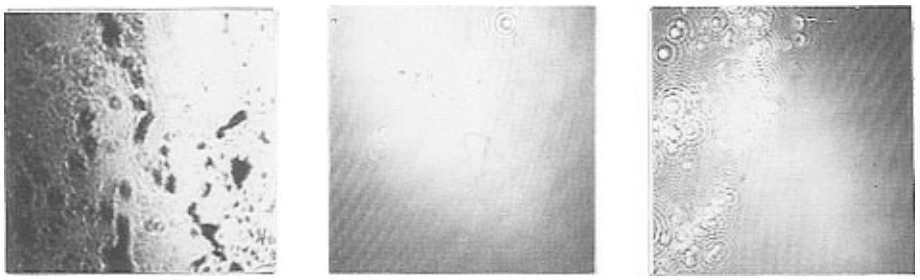

a b c

Figure 4. Brewster angle microscopy during compression of **2** (see Figure 3) on pure water at 20 °C at a surface pressure of (a) 0 mN/m, (b) 10 mN/m, and (c) > 60 mN/m (magnification: horizontally, 0.95 cm = 100 μm; vertically, 0.7 cm = 100 μm).

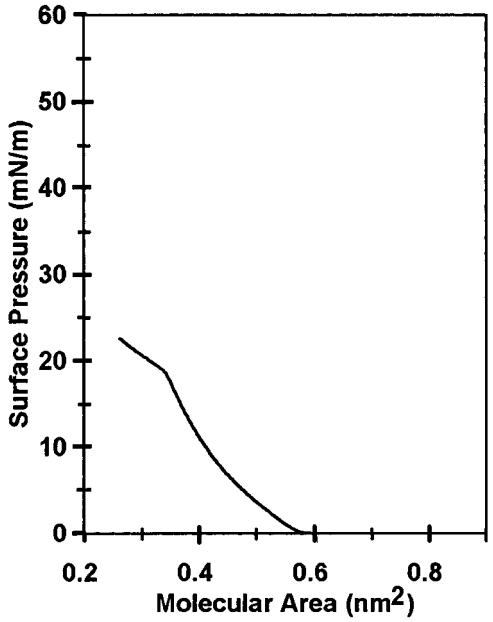

Figure 5. Surface pressure *versus* molecular area isotherm of **3** on aqueous NaCl (10^{-3} M) subphase at 25 °C.

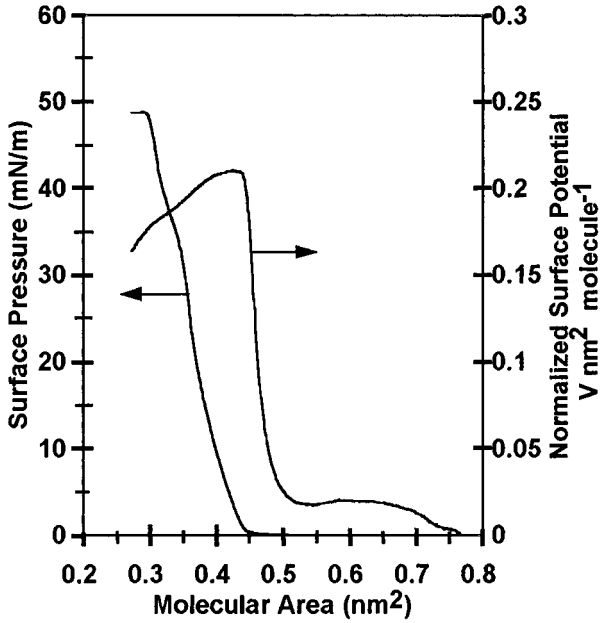

Figure 6. Surface pressure and normalized surface potential *versus* molecular area isotherms of **3**/octadecane (1:1 molar ratio) on aqueous NaCl (10^{-3} M) subphase at 25 °C.

and revealed a lower film quality for **4**. This is in agreement with the fact that lower transfer ratios were obtained in the case of **4** than for **1**, **2**, and **3**/octadecane

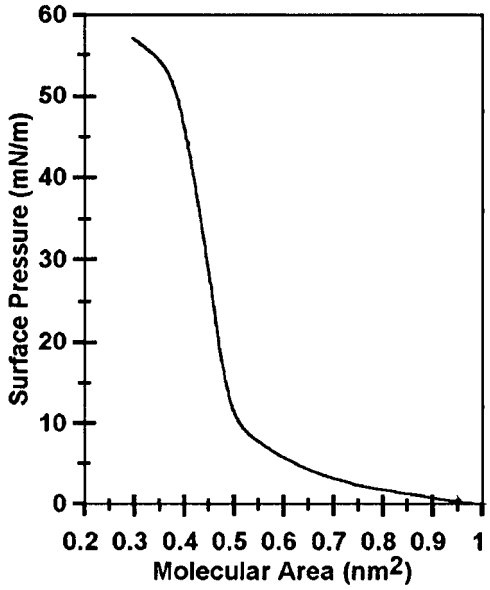

Figure 7. Surface pressure *versus* molecular area isotherm of **4** on pure water at 20 °C (similar behavior was observed at 25 °C).

(see below). The behavior of **4** was not investigated further. Thirdly, hysteresis experiments were carried out with **3**/octadecane. Compression−expansion cycles showed almost no hysteresis if the monolayer was not compressed above 40 mN/m. Finally, the fact that for **1**, **2** and **3**/octadecane transfer ratios near unity as well as a periodicity in the small-angle X-ray scattering (SAXS) patterns were obtained (see below) are the most convincing arguments which prove that stable and ordered monolayers at the air−water interface were obtained.

The above data suggest that in each case the hydrophilic groups interact with the water surface, and the alkyl chains point away from it. Such interactions are responsible for the formation of stable and ordered monolayers. Comparing the data obtained for **4** with the ones of **1** and **2** suggest that the latter two species orient in a similar way as for **4**, *i.e*, with the two substituents in the *cis*-conformation. In the case of **3**, the two substituents are most likely in the *trans*-conformation to favor interactions between the alcoholic function and the water surface. Finally, the variation of the normalized surface potential of **1**, **2**, and **3**/octadecane indicates different behavior of **1** with respect to **2** and **3**/octadecane during the film formation. This should be related to (1) the nature and number of the substituents located on the ferrocene and (2) stronger hydrophilic interactions with the subphase in the case of **1** which bears two polar head groups.

Langmuir-Blodgett Films. Y-Type transferred films (downward and upward deposition mode) of **1**, **2,** and **3**/octadecane (1:1) were successfully prepared onto hy-

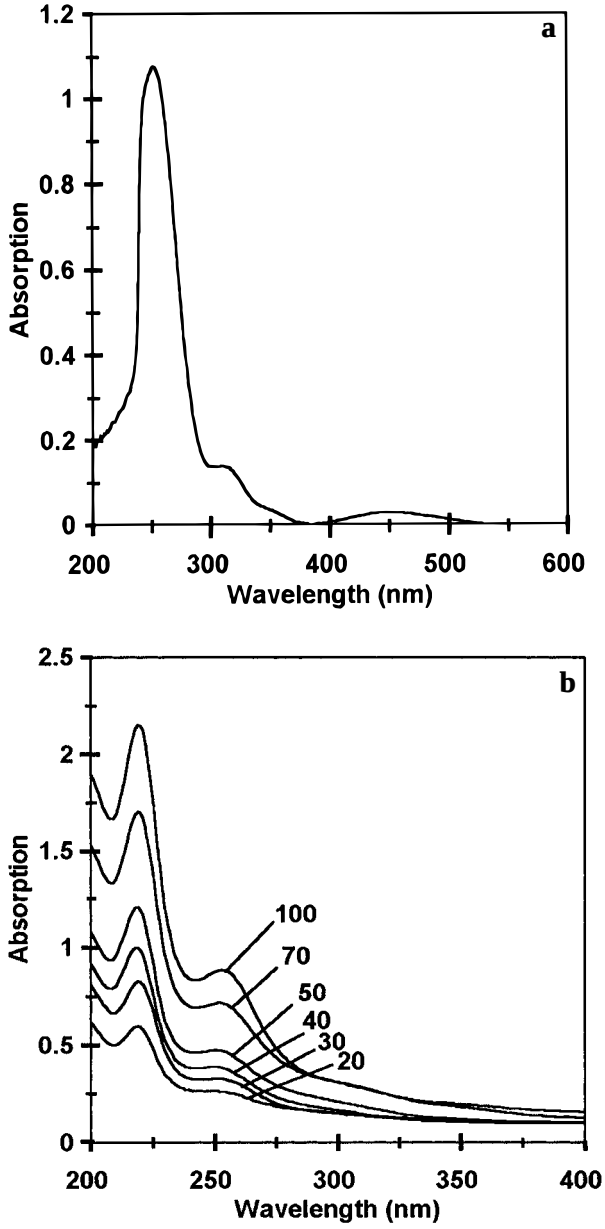

Figure 8. The UV−vis spectra of **1** in (a) $CHCl_3$ solution (1.02×10^{-4} mol/L), and (b) onto hydrophobized quartz plates (the number of transferred layers is indicated on the figure).

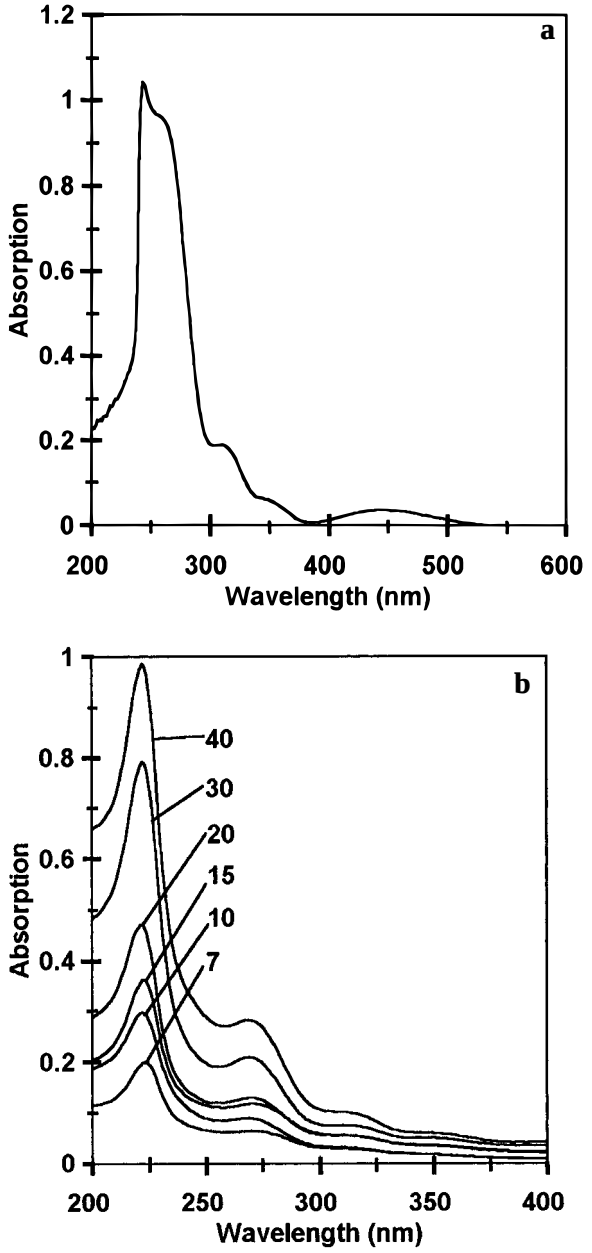

Figure 9. The UV−vis spectra of **2** in (a) $CHCl_3$ solution (1.20×10^{-4} mol/L), and (b) onto hydrophobized quartz plates (the number is of transferred layers is indicated on the figure).

drophobized quartz or glass substrates using the conventional dipping method (see Experimental Section). In each case, a transfer ratio close to unity was obtained. Up to 100 monolayers could be transferred for **1**; in the case of **2** and **3**/octadecane (1:1), 60 and 30 monolayers could be deposited, respectively; these values do not represent an upper limit. To ensure high quality of the transferred films, the monolayer (at the air−water interface) was renewed every 20 transfers. The LB films were characterized by UV−vis spectroscopy and small-angle X-ray scattering (SAXS). Transfer of monolayers from ferrocenophane derivative **4** was more difficult (lower transfer ratios were obtained for **4** than for **1**, **2**, and **3**/octadecane). This result may reflect a destabilization of the monolayer organization during the transfer process because of the trimethylene unit. Langmuir−Blodgett film formation from **4** was therefore not investigated.

UV−vis Spectroscopy. Films were deposited onto quartz plates pretreated with octadecyltrichlorosilane. The UV spectra of **1**, **2** and **3**/octadecane (1:1) in chloroform solution and for the transferred films are reported in Figures 8, 9, and 10, respectively.

In solution, typical absorption bands of the ferrocenyl core were observed at 450 and 250 nm.[4] In the case of transferred films, a blue shift of the absorption peaks was observed as compared with solution spectra. Such behavior was already reported for other ferrocene derivatives[7b] and was attributed to the formation of H-aggregates.[13] A linear increase of the absorption was detected with the number of layers indicating that **1**, **2**, and **3**/octadecane (1:1) were transferred quantitatively and effectively. The chemical stability of the transferred films was evaluated by measuring the variation of the absorption maximum as a function of time. A decrease of about 1% and a blue shift of 2 nm for the maximum absorption peak were observed 4 days after deposition. No further modifications were noticed several months

(13) Evans, C. E.; Song, Q.; Bohn, P. W. *J. Phys. Chem.* **1993**, *97*, 12302.

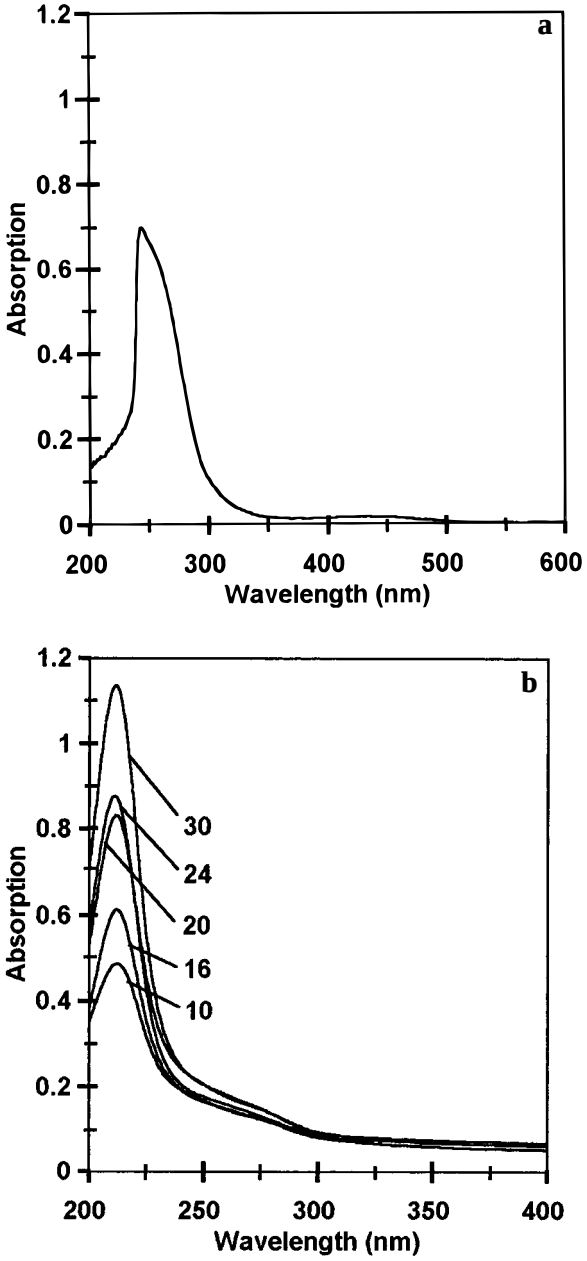

Figure 10. The UV−vis spectra of **3**/octadecane (1:1 molar ratio) (a) in $CHCl_3$ solution (1.30×10^{-4} mol/L) and (b) onto hydrophobized quartz plates (the number of transferred layers is indicated on the figure).

later, which indicated good chemical stability of the deposited films.

Small-Angle X-ray Scattering. SAXS experiments were conducted for films which were deposited onto glass plates pretreated with octadecyltrichlorosilane.

The diffractograms for 12 layers of **1**, **2**, and **3**/octadecane (1:1) recorded 4 days and 2 months after deposition are presented in Figures 11, 12 and 13, respectively. Sharp diffraction signals were observed; second-order [for **3**/octadecane (1:1)] and second- and third-order (for **1** and **2**) diffraction peaks were detected. These data proved the formation of highly ordered and stable LB films.

Figure 14 shows the evolution of the diffraction pattern for six layers of **2**, 1 day, 4 days, and 2 months after deposition. Only one diffraction peak was observed at $2\theta = 1.93°$ (5.3 nm) 1 day after deposition (Figure 14a). Four days after deposition, a new peak appeared at $2\theta = 2.63°$ (3.9 nm) (Figure 14b), while the first one decreased in intensity. No further modifications were observed as

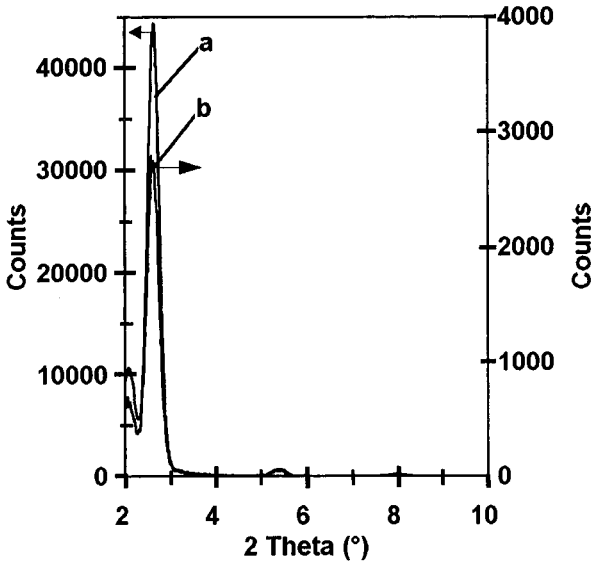

Figure 11. Small-angle X-ray scattering of a 12-layer Langmuir−Blodgett film of **1** onto a hydrophobized glass plate obtained (a) 4 days and (b) 2 months after deposition.

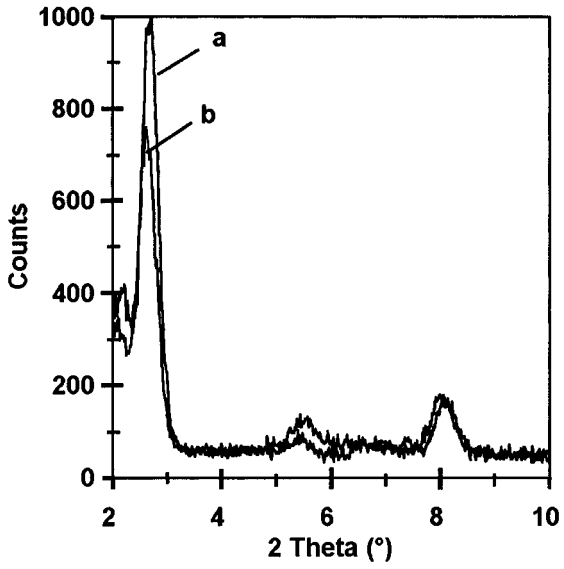

Figure 12. Small-angle X-ray scattering of a 12-layer Langmuir−Blodgett film of **2** onto a hydrophobized glass plate obtained (a) 4 days and (b) 2 months after deposition.

indicated by the diffraction pattern recorded 2 months after deposition (Figure 14c). As expected in the latter case, the diffraction pattern ressembled the one reported in Figure 12. These data are important because they show that the LB film tends to an equilibrium which is reached only a few days after deposition. The variation of the SAXS diffractograms is in agreement with the modification of the UV−vis spectra (see above). The differences between the spectra of **2** displayed in Figures 12 and 14 are a consequence of a higher organization degree for the 12-layer system than for the 6-layer one and a more rapid stabilization process with a higher number of layers. Similar results were obtained for **1** and **3**/octadecane (1:1).

The SAXS experiments are of particular interest as they give information regarding the arrangement of the molecular units within the organized molecular films. From the diffractograms presented in Figures 11−13, a periodicity of 3.9, 3.8, and 3.3 nm was found for **1**, **2**, and **3**/octadecane (1:1), respectively. These values were attributed to a double layer spacing, *i.e.*, to the distance

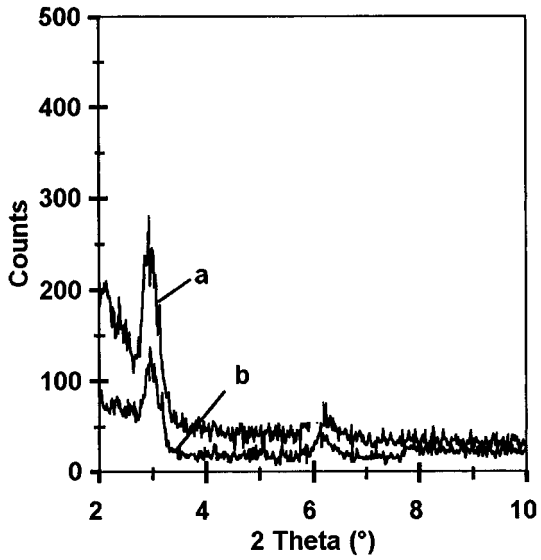

Figure 13. Small-angle X-ray scattering of a 12-layer Langmuir−Blodgett film of **3**/octadecane (1:1 molar ratio) onto a hydrophobized glass plate obtained (a) 4 days and (b) 2 months after deposition.

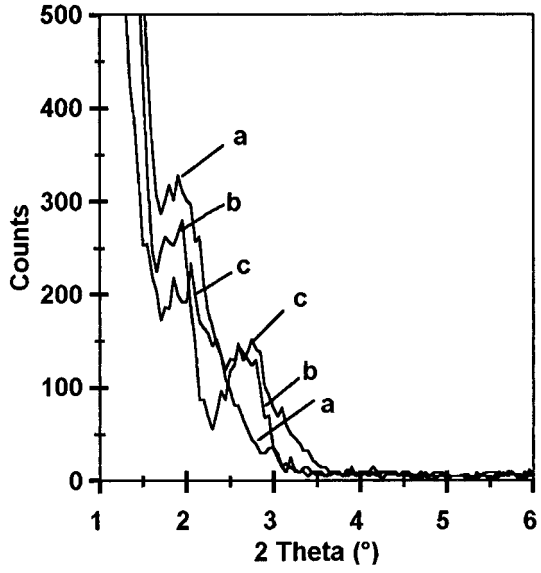

Figure 14. Small-angle X-ray scattering of a 6-layer Langmuir−Blodgett film of **2** onto a hydrophobized glass plate obtained (a) 1 day, (b) 4 days, and (c) 2 months after deposition.

between two ferrocene nuclei separated by alkyl chains. The molecular length in the fully extended chain conformation determined by CPK molecular models was found to be *ca.* 3.0 nm for **1** (*cis* conformation), **2** (*cis* conformation), and **3** (*trans* conformation). Therefore, the above SAXS values indicate that the molecules are tilted within the layers, with a tilt angle of *ca.* 50° for **1**, 51° for **2**, and 56° for **3**/octadecane (1:1). A situation where the ferrocene derivatives would be perpendicular to the layers forming a bilayer can be excluded; a SAXS periodicity of 6.0 nm would have been obtained. An interdigitated arrangement is also less likely: firstly, BAM investigations have shown that the chains are tilted on the water surface (comparison of parts e and f of Figure 2 showed that a variation of the polarizor angle led to an opposite contrast (*i.e.*, Figure 2e can be considered as the negative image of Figure 2f));[14] secondly, the layers are too compact to allow interdigitation.

(14) Hönig, D.; Overbeck, G. A.; Möbius, D. *Adv. Mater.* **1992**, *4*, 419.

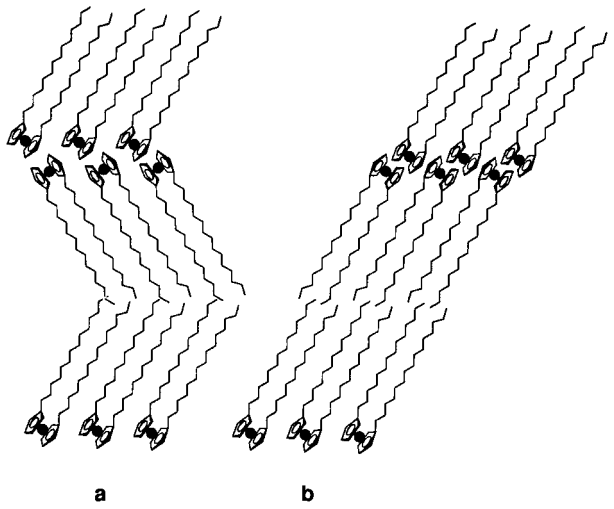

Figure 15. Possible supramolecular organizations of the ferrocene-containing molecular units within the Langmuir−Blodgett films (see text).

Two possible supramolecular arrangements can be postulated for the organization of the investigated molecular units within the LB films (Figure 15). In the first case, the ferrocene derivatives are tilted with respect to the normal of the layers and form a chevron structure (Figure 15a); in the second one, the molecules are tilted and point toward the same direction (Figure 15b). The presence of both organizations is also feasible as already observed for other systems.[15]

The data described in the present report are of particular importance as they show that ordered and stable Langmuir and LB films can be obtained from various ferrocene derivatives. The successful derivatization of the ferrocene unit by two different substitutents opens the way for the design of novel amphiphilic ferrocene-containing molecular building blocks. The possibility of employing an intercalant (octadecane in the present case) is an interesting result for elaborating systems which may combine the characteristics of a ferrocene derivative with those of an intercalant. Interestingly, the substitution pattern may also be used for tuning the redox properties[16] of the ferrocene moiety with the view to constructing electroactive anisotropic molecular films, or to control the supramolecular organization as reported for vesicle formation[17] and, more recently, for liquid-crystalline phase induction.[18]

Conclusion

To understand how polar headgroups and alkyl chains can be combined for obtaining Langmuir and LB films from ferrocene-containing molecular units, we have designed, synthesized, and characterized new amphiphilic ferrocene derivatives. This work has shown that a substitution pattern composed of two hydrophobic chains with either one or two hydrophilic functions led to stable and ordered molecular films, while one hydrophobic chain associated with one hydrophilic headgroup required the presence of an intercalant to fill the space around the

(15) Delamarche, R.; Michel, B.; Gerber, C.; Anselmetti, D.; Güntherodt, H.-J.; Wolf, H.; Ringsdorf, H. *Langmuir* **1994,** *10*, 2869.

(16) Zanello, P. In *Ferrocenes: Homogeneous Catalysis, Organic Synthesis, Materials Science*; Togni, A., Hayashi, T., Eds.; VCH Verlagsgesellschaft: Weinheim, 1995; pp 317−430.

(17) (a) Wang, K.; Munoz, S.; Zhang, L.; Castro, R.; Kaifer, A. E.; Gokel, G. W. *J. Am. Chem. Soc.* **1996,** *118*, 6707. (b) Medina, J. C.; Gay, I.; Chen, Z.; Echegoyen, L.; Gokel, G. W. *J. Am. Chem. Soc.* **1991**, *113*, 365.

(18) Deschenaux, R.; Schweissguth, M.; Levelut, A.-M. *Chem. Commun.* **1996**, 1275.

bulky ferrocene unit. This behavior is in agreement with results reported for ferrocene-containing thermotropic liquid crystals[12] and further emphasizes the key role played by the three-dimensional structure of the ferrocene unit for obtaining organized molecular assemblies. Small-angle X-ray diffraction investigations demonstrated that the LB films tend to an equilibrium situation which is reached a few days after transfer of the monolayers.

Experimental Section

Materials and General Methods. Dichloromethane ($CaCl_2$ and then P_2O_5, under nitrogen) and THF (sodium, under nitrogen) were distilled and dried prior to use. Oxalyl chloride (purum), pyridine (puriss p.a.), benzyl alcohol (puriss p.a.), triethylamine (puriss p.a.), 4-pyrrolidinopyridine (purum), octadecanol (purum), aluminum chloride (puriss), and zinc (pulv., purum) were purchased from Fluka and used as received. Mercury chloride (pro analysis) was purchased from Merck and used as received. Stearoyl chloride (pract.) was purchased from Fluka and distilled prior to use. Ferrocene-1,1′-dicarboxylic acid chloride (**5**),[8] ferrocene carboxylic acid chloride (**6**),[8] and [3]ferrocenophane-3,3′-dicarboxylic acid chloride (**15**)[9] were prepared by following literature procedures. Reactions involving the formation or transformation of acid chloride function(s) were protected from light (aluminum foil) and carried out under nitrogen. Column chromatography: silica gel 60 (0.060−0.200 mm, SDS) or alumina (neutral, type 507C, 100−125 mm, Fluka). Thin layer chromatography: silica gel plates $60F_{254}$ (Merck) or alumina (Merck). Melting points: Büchi 510 instrument (uncorrected). UV spectra: Uvikon 930 spectrophotometer. IR spectra: Perkin-Elmer 1720 FTIR spectrometer. NMR spectra: Bruker AMX 400 and Varian Gemini 200 spectrometers; solvent as an internal reference. Mass spectra (electronic impact): Nermag R 30.10 spectrometer. Elemental analyses were performed by Mikroelementaranalytisches Laboratorium, ETH-Zurich, and Ciba (Marly). Abbreviations: 4-pyrrolidinopyridine = 4-ppy; triethylamine = Et_3N; OTS = octadecyltrichlorosilane.

Langmuir−Blodgett Technique. Instrumentation: KSV Instrument Inc., Finland. Experiments were carried out on a Langmuir trough LB 5000 (Teflon coating, 50 × 15 cm) equipped with two hydrophobic barriers, a Wilhelmy balance as a surface-pressure sensor and a 5000 SP surface-potential meter (vibrating capacitor method). The whole system, fully computer controlled, was placed on an active vibration-isolating table and was protected from dust by a home-made plastic cover.

Film formations were carried out by the ordinary method. Typical conditions were as follows: subphase, water (18 MΩ cm^{-1}; Elgastat UHQ-II, Kleiner, Switzerland); temperature, subphase thermostated within ±0.2 °C, atmosphere at 20−22 °C; concentration and volume of chloroform solution of the amphiphile: 0.8−1.3 mg/mL, 70−150 μL; compression speed, 20 mm/min (*i.e.*, 60 cm^2/min). Vertical transfers were performed at the following surface pressures: **1**, 25 mN/m; **2**, 20 mN/m; **3**/octadecane (1:1), 30 mN/m at a rate of 5 mm/min. To ensure high quality of the transferred films, the monolayer (at the air−water interface) was renewed every 20 transfers. Upper and lower delay: 30 s. Cleaning of the quartz and glass plates: the plates were (i) treated with a 5% RBS solution (Fluka) with an ultrasonic bath at 80 °C for 30 min, (ii) rinsed with UHQ water, MeOH, and UHQ water, (iii) treated in UHQ water with an ultrasonic bath at 80 °C for 30 min, (iv) rinsed with UHQ water, MeOH, and UHQ water, and (v) dried at 140 °C. Hydrophobization of the quartz and glass plates: the cleaned plates were (i) immersed in a solution containing OTS (0.5 mL), decaline (25 mL), $CHCl_3$ (25 mL), and CCl_4 (50 mL) and treated with an ultrasonic bath at 60 °C for 15 min, (ii) rinsed successively with CH_2Cl_2, MeOH, and UHQ water, and (iii) dried at 140 °C.

Brewster-Angle Microscopy. Instrumentation: BAM-1 Brewster-angle microscope (Nanofilm Technologie, Germany).

Small-Angle X-ray Scattering. Instrument: STOE Stadi P powder diffractometer. Focused Co $K\alpha_1$ radiation with λ = 0.178 897 nm was obtained by a curved Ge(111) monochromator. Data were collected in the 0.5−10° 2θ range in reflection mode. The instrument was calibrated with a multilayer system of cadmium arachidate.

1,1′-Dicarbooctadecyloxyferrocene (1). To a solution of ferrocene-1,1′-diacid chloride (**5**) (1.30 g, 4.18 mmol) in CH_2Cl_2 (30 mL) were added a solution of octadecanol (3.39 g, 12.5 mmol) in CH_2Cl_2 (50 mL), 4-ppy (catalytic amount), and Et_3N (0.85 g, 8.4 mmol). The mixture was stirred at room temperature for 16 h, washed with water, dried ($MgSO_4$), and evaporated to dryness. Purification of the residue by column chromatography (alumina, hexane/AcOEt 20:1) and crystallization from EtOH gave pure **1** (0.50 g, 15%). Mp 63−65 °C. UV−vis ($CHCl_3$) nm (ϵ): 251 (10 540), 308 (1360), 449 (280). ^{1}H NMR (400 MHz, $CDCl_3$) δ: 4.82 (m, 4 H, HCp), 4.39 (m, 4 H, HCp), 4.21 (t, 4 H, CH_2O), 1.73 (m, 4 H, CH_2CH$_2$O), 1.25 (br s, 60 H, aliphatic CH_2), 0.88 (t, 6 H, CH_3). ^{13}C NMR (100 MHz, $CDCl_3$) δ: 170.59, 73.19, 72.89, 71.51, 64.68, 31.98, 29.76, 29.41, 28.91, 28.11, 22.74, 14.18. IR (KBr): 2917, 2850, 1720, 1293, 1159. Anal. Calcd for $C_{48}H_{82}O_4Fe$ (779.02): C, 74.00; H, 10.61. Found: C, 74.03; H, 10.63.

Carbobenzyloxyferrocene (7). To a solution of ferrocene-carboxylic acid chloride **6** (5.4 g, 22 mmol) in CH_2Cl_2 (70 mL) were added Et_3N (2.2 g, 22 mmol) and benzyl alcohol (2.7 g, 25 mmol). The solution was stirred at room temperature for 4 h, diluted with CH_2Cl_2 (100 mL), washed with water, dried ($MgSO_4$) and evaporated to dryness. Purification of the residue by column chromatography (silica gel, hexane/AcOEt 5:1) gave pure **7** (4.8 g, 68%). Mp 84−86 °C. ^{1}H NMR (200 MHz, $CDCl_3$) δ: 7.45 (m, 5 H, benzyl), 5.27 (s, 2 H, CH_2), 4.86 (br s, 2 H, HCp), 4.41 (br s, 2 H, HCp), 4.13 (br s, 5 H, HCp). ^{13}C NMR (100 MHz, $CDCl_3$) δ:172.16, 137.30, 129.24, 129.00, 128.87, 72.11, 71.79, 70.94, 70.44, 66.52. IR (KBr): 3980, 3087, 3029, 2973, 1702, 1458, 1376, 1275.

1-Carbobenzyloxy-1'-octadecanoylferrocene (8). Powdered zinc (8.1 g, 0.12 mol) and $AlCl_3$ (3.6 g, 27 mmol) were added to a stirred solution of **7** (4.0 g, 12.5 mmol) in CH_2Cl_2 (150 mL) cooled to 0 °C. Stearoyl chloride (8.3 g, 27 mmol) in CH_2Cl_2 (50 mL) was added dropwise over a period of 10 min. The reaction mixture was stirred at 0 °C for 2 h, filtered, diluted with CH_2Cl_2, and hydrolyzed with water. The organic layer was washed with a diluted aqueous $NaHCO_3$ solution, dried ($MgSO_4$), and evaporated to dryness. Purification of the residue by column chromatography (silica gel, hexane/AcOEt 10:1) and crystallization from EtOH gave pure **8** (4.7 g, 64%). Mp 70−71 °C. ^{1}H NMR (400 MHz, $CDCl_3$) δ: 7.40 (m, 5 H, benzyl), 5.23 (s, 2 H, CH_2-benzyl), 4.82 (t, 2 H, HCp), 4.68 (t, 2 H, HCp), 4.39 (t, 2 H, HCp), 4.36 (t, 2 H, HCp), 2.61 (t, 2 H, CH_2CH_2CO), 1.64 (m, 2 H, CH_2CH$_2$CO), 1.26 (br s, 28 H, aliphatic CH_2), 0.88 (t, 3 H, CH_3). ^{13}C NMR (100 MHz, $CDCl_3$) δ: 204.03, 170.88, 136.93, 129.29, 129.26, 129.05, 74.07, 73.50, 73.37, 72.22, 71.29, 66.92, 40.52, 32.60, 30.38, 30.34, 30.25, 30.16, 30.04, 25.02, 23.37, 14.79. Anal. Calcd for $C_{36}H_{50}O_3Fe$ (586.64): C, 73.71; H, 8.59. Found: C, 73.79; H, 8.61.

1-Carbobenzyloxy-1'-octadecylferrocene (9). A mixture of powdered zinc (2.0 g, 31 mmol), $HgCl_2$ (0.15 g, 0.55 mmol), water (2.5 mL), and concentrated HCl (0.1 mL) was stirred at room temperature for 5 min. The upper layer was eliminated by means of a pipet and replaced by water (5 mL) and concentrated HCl (1.5 mL). A solution of **8** (0.3 g, 0.5 mmol) in toluene (6 mL) was added and the mixture stirred under reflux for 24 h. At this stage, concentrated HCl (1 mL) was added and the mixture stirred under reflux for a further 6 h. The organic layer was recovered, diluted with toluene, washed with water to neutral pH, dried ($MgSO_4$) and evaporated to dryness. Crystallization of the residue from EtOH gave pure **9** (0.28 g, 98%). Mp 45−50 °C. ^{1}H NMR (200 MHz, $CDCl_3$) δ: 7.4 (m, 5 H, benzyl), 5.27 (s, 2 H, CH_2-benzyl), 4.75 (t, 2 H, HCp), 4.33 (t, 2 H, HCp), 3.92 (s, 4 H, HCp), 2.2 (t, 2 H, CH_2Cp), 1.65 (m, 2 H, CH_2CH$_2$Cp), 1.26 (br s, 30 H, aliphatic CH_2), 0.89 (t, 3 H, CH_3). ^{13}C NMR (100 MHz, $CDCl_3$) δ: 172.13, 137.24, 129.21, 129.06, 128.83, 77.90, 72.83, 72.17, 71.60, 70.58, 69.72, 66.50, 31.78, 30.38, 30.34, 30.31, 30.27, 30.18, 30.11, 30.04, 29.92, 29.75, 29.32, 23.37, 14.79. IR (KBr): 2913, 2849, 1715, 1635, 1472, 1277, 1133, 1025, 716, 492.

1-Carboxy-1'-octadecylferrocene (10). A mixture of **9** (0.28 g, 0.49 mmol), Pd(10%)/C (catalytic amount) and CH_2Cl_2 (200 mL) was hydrogenated at room temperature under 4.5 bar of hydrogen for 4 h. The solution was filtered and evaporated to dryness. Crystallization of the residue from EtOH gave pure **10** (0.17 g, 72%). Mp 77−79 °C (dec). ^{1}H NMR (200 MHz, $CDCl_3$) δ: 4.77 (t, 2 H, HCp), 4.41 (t, 2 H, HCp), 4.13 (s, 4 H, HCp), 2.29 (t, 2 H, CH_2Cp), 1.50 (m, 2 H, CH_2CH$_2$Cp), 1.26 (br s, 30 H,

aliphatic CH_2), 0.89 (t, 3 H, CH_3). ^{13}C NMR (100 MHz, $CDCl_3$) δ: 178.99, 91.95, 73.20, 71.79, 70.69, 69.94, 32.61, 31.75, 30.39, 30.35, 30.32, 30.22, 30.05, 29.02, 23.37, 14.80. Anal. Calcd for $C_{29}H_{46}O_2Fe$ (482.53): C, 72.19; H, 9.61. Found: C, 72.25; H, 9.66.

1-Carbooctadecyloxy-1'-octadecylferrocene (2). A solution of **10** (0.14 g, 0.29 mmol), oxalyl chloride (0.38 g, 3.0 mmol), and pyridine (a few drops) in CH_2Cl_2 (5 mL) was heated under reflux for 5 h, cooled to room temperature, and evaporated to dryness. The solid residue was extracted several times with hot petroleum ether (bp = 60−90 °C). Combination of the organic extracts and evaporation to dryness gave 1-chlorocarboxy-1′-octadecylferrocene (**11**) (0.145 g, 100%) which was used in the next step without further purification.

To **11** (0.14 g, 0.28 mmol) in CH_2Cl_2 (5 mL) were added a solution of octadecanol (0.12 g, 0.44 mmol) in CH_2Cl_2 (5 mL), Et_3N (58 mg, 0.57 mmol), and 4-ppy (catalytic amount). The mixture was stirred under reflux overnight, cooled to room temperature, washed with water, dried ($MgSO_4$), and evaporated to dryness. Purification of the residue by column chromatography (silica gel, hexane/AcOEt 10:1) and crystallization from EtOH gave pure **2** (0.14 g, 68%). Mp 68−69 °C. UV−vis ($CHCl_3$) nm (ϵ): 242 (8680), 309 (1580), 445 (300). ^1H NMR (400 MHz, $CDCl_3$) δ: 4.73 (s, 2 H, HCp), 4.33 (s, 2 H, HCp), 4.18 (t, 2 H, CH_2O), 4.09 (s, 4 H, HCp), 2.24 (t, 2 H, CH_2Cp), 1.71 (m, 2 H, CH_2CH_2O), 1.43 (m, 2 H, CH_2CH_2Cp), 1.26 (br s, 60 H, aliphatic CH_2), 0.88 (t, 6 H, CH_3). ^{13}C NMR (100 MHz $CDCl_3$) δ: 172.35, 91.90, 72.70, 72.52, 71.42, 70.52, 69.63, 64.96, 32.61, 31.81, 30.39, 30.35, 30.26, 30.21, 30.05, 29.63, 29.34, 26.82, 23.37, 14.79. IR (KBr): 2917, 2850, 1698, 1661, 1471, 1457, 1276, 1147, 1038. Anal. Calcd for $C_{47}H_{82}O_2Fe$ (735.00): C, 76.80; H, 11.24. Found: C, 76.74; H, 11.38.

Carbomethoxyferrocene (12). A solution of **6** (0.5 g, 2 mmol), Et_3N (0.4 g, 4 mmol), 4-ppy (catalytic amount), and MeOH (1.0 mL, 25 mmol) in CH_2Cl_2 (15 mL) was heated under reflux for 3 h, cooled to room temperature, and filtered over silica gel (10 g, CH_2Cl_2). Evaporation of the solvent gave pure **12** (0.49 g, 100%). Mp 68−70 °C. ^1H NMR (400 MHz, $CDCl_3$) δ: 4.80 (s, 2 H, HCp), 4.39 (s, 2 H, HCp), 4.20 (s, 5 H, unsubst. Cp), 3.80 (s, 3 H, CH_3). ^{13}C NMR (100 MHz, $CDCl_3$) δ: 172.87, 71.94, 71.77, 70.79, 70.41, 52.23. IR (KBr): 2923, 1713, 1702, 1466, 1375, 1281, 1190, 1140, 824.

1-Carbomethoxy-1′-octadecanoylferrocene (13). Powdered zinc (1.3 g, 20 mmol) and $AlCl_3$ (0.33 g, 2.5 mmol) were added to a stirred solution of **12** (0.5 g, 2 mmol) in CH_2Cl_2 (20 mL) cooled to 0 °C. Stearoyl chloride (0.75 g, 2.5 mmol) in CH_2Cl_2 (5 mL) was added over a period of 10 min. The reaction mixture was stirred at 0 °C for 3 h and hydrolyzed with water (20 mL). The organic layer was recovered, filtered, washed with a saturated aqueous $NaHCO_3$ solution, dried ($MgSO_4$), and evaporated to dryness. Crystallization of the residue from EtOH gave pure **13** (0.90 g, 88%). Mp 79−81 °C. ^1H NMR (400 MHz, $CDCl_3$) δ: 4.80 (t, 2 H, HCp), 4.78 (t, 2 H, HCp), 4.49 (t, 2 H, HCp), 4.40 (t, 2 H, HCp), 3.82 (s, 3 H, CH_3O), 2.67 (t, 2 H, CH_2CO), 1.68 (m, 2 H, CH_2CH_2CO), 1.25 (br s, 28 H, aliphatic CH_2), 0.88 (t, 3 H, CH_3CH_2). ^{13}C NMR (100 MHz, $CDCl_3$) δ: 204.42, 171.50, 81.12, 74.02, 73.51, 73.32, 72.18, 71.38, 52.42, 40.59, 32.61, 30.39, 30.35, 30.25, 30.21, 30.05, 25.02, 23.38, 14.81. IR (KBr): 2916, 2849, 1715, 1660, 1472, 1376, 1285, 1149, 491. Anal. Calcd for $C_{30}H_{46}O_3Fe$ (510.54): C, 70.58; H, 9.08. Found: C, 70.70; H, 9.18.

1-Carbomethoxy-1'-octadecylferrocene (14). A mixture of granular zinc (2.0 g, 31 mmol), $HgCl_2$ (0.15 g, 0.55 mmol), water (2.5 mL), and concentrated HCl (0.5 mL) was stirred at room temperature for 5 min. The aqueous phase was eliminated with a pipet and replaced by water (5 mL) and concentrated HCl (2 mL). A solution of **13** (0.30 g, 0.59 mmol) in toluene (10 mL) was added. The suspension was heated under reflux for 3 h. The organic phase was recovered, diluted with toluene, washed with water to neutral pH, dried ($MgSO_4$), and evaporated to dryness. Crystallization of the residue from EtOH gave pure **14** (0.22 g, 75%). Mp 55−56 °C. ^1H NMR (200 MHz, $CDCl_3$) δ: 4.72 (t, 2 H, HCp), 4.34 (t, 2 H, HCp), 4.08 (s, 4 H, HCp), 3.80 (s, 3 H, CH_3O), 2.25 (t, 2 H, CH_2Cp), 1.50 (m, 2 H, CH_2CH_2Cp), 1.26 (br s, 30 H, aliphatic CH_2), 0.89 (t, 3 H, CH_3CH_2). ^{13}C NMR (100 MHz, $CDCl_3$) δ: 172.72, 91.84, 72.47, 72.21, 71.29, 70.42, 69.55, 52.11, 32.62, 31.79, 30.40, 30.32, 30.26, 30.21, 30.06, 29.22, 23.39, 14.82. IR (KBr): 2919, 2849, 1705, 1469, 1278, 1141. Anal. Calcd for $C_{30}H_{48}O_2Fe$ (496.55): C, 72.57; H, 9.74. Found: C, 72.56; H, 9.67.

1-Hydroxymethyl-1′-octadecylferrocene (3). A spatula tip of $LiAlH_4$ was added to a solution of **14** (0.20 g, 0.40 mmol) in THF (20 mL) cooled to 0 °C. The mixture was stirred for 30 min, hydrolyzed with water, and diluted with diethyl ether. The organic layer was washed with water to neutral pH, dried ($MgSO_4$), and evaporated to dryness. Crystallization of the residue from heptane gave pure **3** (0.15 g, 80%). Mp 57−59 °C. UV−vis ($CHCl_3$) nm (ϵ): 243 (6670). ^1H NMR (200 MHz, $CDCl_3$) δ: 4.33 (br d, 2 H, CH_2OH; s when D_2O was added), 4.16 (t, 2 H, HCp), 4.12 (t, 2 H, HCp), 4.07 (s, 4 H, HCp), 2.30 (t, 2 H, CH_2Cp), 1.50 (m, 2 H, CH_2CH_2Cp), 1.26 (br s, 30 H, aliphatic CH_2), 0.89 (t, 3 H, CH_3). ^{13}C NMR (100 MHz, $CDCl_3$) δ: 70.08, 69.47, 68.33, 61.41, 32.61, 31.92, 30.39, 30.31, 30.27, 30.21, 30.13, 30.05, 23.38, 14.81. IR (KBr): 3314, 2918, 2851, 1473, 1466, 1042, 1024, 993. Anal. Calcd for $C_{29}H_{48}OFe$ (468.54): C, 74.34; H, 10.33. Found: C, 74.58; H, 10.49.

1,1'-Trimethylene-3,3'-carbooctadecyloxyferrocene (4). *n*-BuLi (16.6 mL, 1.6 M in hexane) was added to a solution of octadecanol (6.9 g, 26 mmol) in THF (150 mL). The mixture was stirred at room temperature for 1 h and 30 min and then cooled to −50 °C. A solution of **15** (1.0 g, mixture of mono- and diacid chlorides) in THF (30 mL) was added and the mixture stirred while the temperature raised slowly to room temperature. The mixture was stirred at room temperature for 1 h, under reflux for 2 h, cooled to room temperature, and diluted with water and CH_2Cl_2. The organic layer was washed with water, dried ($CaCl_2$), and evaporated to dryness. The residue was chromatographed through a silica gel column with pentane/diethyl ether 9:1 as the eluent. The mixture contained six compounds: two monoester derivatives (R_f (silica gel, pentane/diethyl ether 9:1) = 0.47 and 0.40, MS: 523 ($M^+ + 1$), 522 (M^+)) and four diester derivatives among which the desired **4** (0.28 g) (R_f (silica gel, pentane/diethyl ether 9:1) = 0.14) was isolated; the yield of the reaction cannot be given as the proportion of the starting mono- and diacid chlorides is not known. Mp 67−69 °C. ^1H NMR (400 MHz, $CDCl_3$) δ: 4.80 (m, 4 H, $H_{(2,2',4,4')}$), 4.13 (m, 2 H, $H_{(5,5')}$), 4.12 (t, 4 H, CH_2O), 2.1−1.8 (m, 6 H, $H_{(6,7,8)}$), 1.67 (m, 4 H, CH_2CH_2O), 1.25 (br s, 60 H, aliphatic CH_2), 0.88 (t, 6 H, CH_3). ^1H NMR (400 MHz, acetone-d_6) δ: 4.91 (t, J_m = 1.3 Hz, 2 H, $H_{(2,2')}$), 4.85 (dd, J_o = 2.5 Hz, J_m = 1.3 Hz, 2 H, $H_{(4,4')}$), 4.42 (dd, J_o = 2.5 Hz, J_m = 1.3 Hz, 2 H, $H_{(5,5')}$), 4.21 (t, J = 6.8 Hz, 4 H, CH_2O), 2.3−2.0 (m, 6 H, $H_{(6,7,8)}$), 1.83−1.77 (m, 4 H, CH_2CH_2O), 1.41 (br s, 60 H, aliphatic CH_2), 1.0 (t, J = 6.7 Hz, 6 H, CH_3). ^{13}C NMR (100 MHz, $CDCl_3$) δ: 169.53 (CO); 89.17 ($C_{(3,3')}$); 74.93 ($C_{(1,1')}$); 72.85 ($C_{(5,5')}$); 71.73 ($C_{(2,2')}$); 70.99 ($C_{(4,4')}$); 64.46 (CH_2O); 34.94 ($C_{(6,7,8)}$); 31.98, 29.77, 29.65, 29.42, 28.81, 26.07, 24.16, 22.75 (aliphatic CH_2); 14.18 (CH_3). IR (KBr): 2916, 2850, 1723, 1295, 1216, 1187. MS: 818 (M^+). Anal. Calcd for $C_{51}H_{86}O_4Fe$ (819.08): C, 74.79; H, 10.58. Found: C, 74.95; H, 10.74.

Chart 2

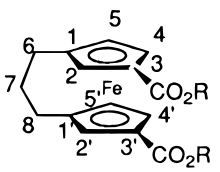

Acknowledgment. R. D. acknowledges the Swiss National Science Foundation for financial support (grant 20−39′485.93) and Ciba (Marly) for elemental analyses.

Supporting Information Available: NMR data (short range and long range HETCOR spectra) of compound **4** (7 pages). Ordering information is given on any current masthead page.